DOI 10.1007/s11182-017-1118-3

Russian Physics Journal, Vol. 60, No. 4, August, 2017 (Russian Original No. 4, April, 2017)

MEAN FREE PATH OF DIFFERENT SEGMENTS OF THE DISLOCATION LOOP IN FCC SINGLE CRYSTALS

R. I. Kurinnaya, M. V. Zgolich, D. N. Cherepanov, and V. A. Starenchenko UDC 548.4

Numerical value of the shear zone diameter is refined. It is assumed that the shear zone is bounded by long strong dislocation barriers formed in the course of reaction between glissile dislocation segments of the loop and dislocations of non-coplanar sliding systems. Based on the modified model of inter-dislocation contact interactions, the mean free path and the probabilities of occurrence of long strong junctions formed by arbitrary components of the dislocation loop are determined. Results are obtained for different orientations of the crystal deformation axes.

Keywords: shear zone, mean free path, reacting dislocations, long strong dislocation junctions, stress of dislocation junction destruction, indestructible dislocation junctions.

INTRODUCTION

One of the problems of mathematical modeling of plastic shear deformation is estimation of the shape and diameter of the shear zone. In [1, 2] methods of theoretical estimation of the shear zone diameter D based on the assumption that the mean free path of the dislocation is determined by reacting dislocations of non-coplanar sliding systems were suggested. The mean free path of dislocations and, hence, the configuration of the shear zone are determined by the probability β_r of forming dislocation junctions [2]. Values of the probability of forming dislocation junctions β_r for dislocations of different orientations were obtained in [3] for the simplest model [4] of reacting dislocation interaction. Schoeck and Frydman [4] used a number of simplifying assumptions to calculate the strength of dislocation junctions because of the complexity of the problem. The simplest model was widely used to calculate the strength of the dislocation junctions softening those or other simplifying assumptions.

It should be noted that the limiting capabilities of the simplest model make it impossible to solve the following problems: 1) to consider arbitrary intersection of reacting dislocations rather than their intersection strictly in the middle, 2) to trace the change of the geometry of dislocation configurations under stress, 3) to determine the length of dislocation barriers, and 4) to determine directly the stress of junction destruction.

In this connection, we have proposed a 3D model of contact inter-dislocation interactions [5, 6] that allows us to describe the dislocation configuration formed in the course of reaction for the actual three-dimensional pattern of intersection of dislocations of non-coplanar sliding systems and to solve the above formulated problem. The 3D model allows the parameters for estimation of the shear zone diameter to be refined and hence a more realistic average diameter of the shear zones to be obtained.

In [7] a more exact method for estimating the shear zone diameter was suggested based on the assumption that the shear zone can be bounded by long strong barriers that can stop various segments of the expanding dislocation loops. As a result, the following expression for the shear zone diameter was obtained:

Tomsk State University of Architecture and Building, Tomsk, Russia, e-mail: riklaz@mail.ru; mzgolich@mail.ru; d_n_ch@mail.ru; star@tsuab.ru. Translated from Izvestiya Vysshikh Uchebnykh Zavedenii, Fizika, No. 4, pp. 67–72, April, 2017. Original article submitted January 27, 2017.

$$D = 2(\beta_D \beta_r \xi \rho)^{-1/2}, \quad (1)$$

where ρ is the shear-forming dislocation density, $\xi = \rho_f \rho^{-1} \approx 0.5$ is the fraction of forest dislocations, ρ_f is the forest dislocation density, and β_r is the probability of forming dislocation junctions. The value of the parameter β_D [7] characterizing the probability of occurrence of a long strong junction is determined for the 3D-model inter-dislocation interactions.

To estimate the number of point defects generated in the course of motion of the dislocation loop, it is necessary to know the mean free path of screw segments of dislocation loops. The shear zone diameter D as a product of the mean free path of dislocations with screw and edge orientations was obtained in [8]:

$$D = \Gamma_D \sqrt{L_S L_E}\ . \quad (2)$$

Here L_S is the length of segments of screw orientation, L_E is the length of segments of edge orientation, and Γ_D is the geometric multiplier depending on the final shape of the shear zone. The mean free path of the loop segment with the *i*th orientation can be calculated from the formula [9]

$$L_i = 2(\beta_D^i \beta_r^i \xi \rho)^{-1/2}, \quad (3)$$

where β_r^i and β_D^i are the parameters of junctions formed by the *i*th component of the dislocation loop.

The present work is aimed at determination of the parameters β_D^i characterizing the probability of forming long strong dislocation junctions by different segments of the expanding dislocation loop for the modern model of inter-dislocation interactions [5, 6].

1. MODELING OF THE CHANGE IN THE DISLOCATION CONFIGURATION UNDER STRESS

As a result of reaction between dislocations of non-coplanar sliding systems, the configuration comprising a dislocation junction is formed (Fig. 1). The model of contact inter-dislocation interactions suggested in [5, 6] allows the change of all dislocation configurations to be investigated under stress rather than of one triple dislocation node as was accepted previously in the simplest model [4]. Changes in the length of dislocation junctions under stress and conditions of destruction of junctions were thus determined. In [5, 6, 10–12] the destruction stress was determined directly by modeling without introduction of any additional intermediate parameters that was characteristic for the simplest model. The intersection of reacting dislocations was considered in any arbitrary point rather than in the middle, as in [4], and this point corresponded to actual intersection of dislocations.

The geometry of the dislocation configuration formed in the course of the dislocation reaction is shown in Fig. 1. The reacting dislocation PQ glissile in the primary plane (d) is intersected with the forest dislocation MN of the secondary plane (c), forming the dislocation junction EF along the line of intersection of the sliding planes. The equilibrium position of the triple dislocation node will correspond to the minimal energy of the entire dislocation configuration provided that the work of external forces is equal to zero $(\tau = 0)$.

Under the external stress τ the dislocation configuration is rearranged occupying a new equilibrium position. The triple dislocation nodes E and F under the action of the applied stress τ are displaced along the line of dislocation junction, occupying new positions K and L, respectively; this leads to enclosing of the areas S_i with the corresponding segments of glissile dislocations $(QE, NE, MF, \text{and } PF)$.

According to [5, 6], we write down the function $F(y_1, y_2)$ that determines the total energy of the dislocation configuration formed under the applied stress in the form

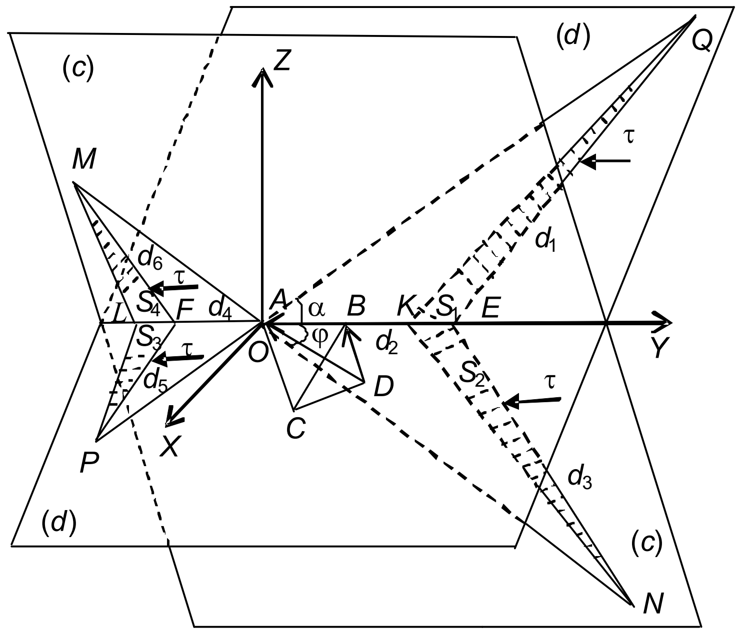

Fig. 1. Geometry of dislocation configurations in the *XYZ* system of coordinates. Here O is the point of intersection of the glissile dislocation *PQ* and the forest dislocation *MN*, EF is the initial length of the junction, KL is the length of the junction under stress τ, d_i ($i = \overline{1,6}$) are the lengths of dislocation segments after formation of the junction, S_i is the area enclosed by the corresponding segment $(QE, NE, MF, \text{or } PF)$, and *ABCD* is the Thompson tetrahedron.

$$F(y_1, y_2) = E_1(y_1)\, d_1(y_1) + E_2(y_1)\, d_2(y_1) + E_3(y_1)\, d_3(y_1)$$

$$+E_4(y_2)\, d_4(y_2) + E_5(y_2)\, d_5(y_2) + E_6(y_2)\, d_6(y_2) \tag{4}$$

$$-\tau\, b(S_1(y_1) + S_2(y_1) + S_3(y_2) + S_4(y_2)).$$

Here the last term describes the work done by the applied stress τ, S_i is the area enclosed with the corresponding segments $(QE, NE, MF, \text{and } PF)$, b is the modulus of the Burgers vector of the glissile dislocation, $d_i(y_1)$ are the lengths and $E_i(y_1)$ are the intrinsic energies per unit length of the corresponding dislocation segments $(QE, OE, \text{and } NE)$, and $d_i(y_2)$ are the lengths and $E_i(y_2)$ are the intrinsic energies per unit length of the corresponding segments $(PF, OF, \text{and } MF)$.

The equilibrium state of the dislocation configurations at the given value of the applied stress τ determines the position of the dislocation nodes K and L (Fig. 1). The minimal energy of the dislocation configuration is determined by the minimum of the function $F(y_1, y_2)$. According to [11], values of the arguments y_1 and y_2 corresponding to this minimum can be determined from the necessary and sufficient condition of the minimum of the function $F(y_1, y_2)$:

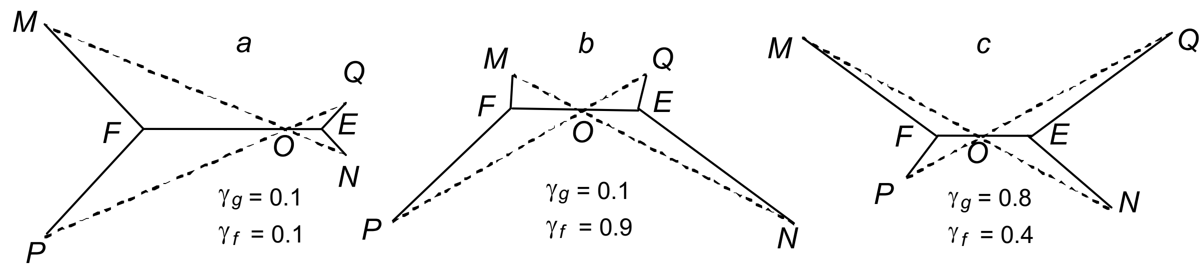

Fig. 2. Arbitrary intersections of the reacting dislocations. The ratio of lengths of glissile dislocation segments is determined by the parameter $\gamma_g = QO / QP = 0.1 - 0.9$. The ratio of lengths of forest dislocation segments is determined by the parameter $\gamma_f = NO/NM = 0.1 - 0.9$. O is the point of intersection of the reacting dislocations. The following values of the parameters were used: *a*) $\gamma_g = 0.1$ and $\gamma_f = 0.1$, *b*) $\gamma_g = 0.1$ and $\gamma_f = 0.9$, and *c*) $\gamma_g = 0.8$ and $\gamma_f = 0.4$.

$$\begin{cases} \dfrac{\partial F(y_1, y_2)}{\partial y_1} = 0, \quad \dfrac{\partial F(y_1, y_2)}{\partial y_2} = 0, \\[2ex] \dfrac{\partial^2 F(y_1, y_2)}{\partial {y_1}^2} \dfrac{\partial^2 F(y_1, y_2)}{\partial {y_2}^2} - \left(\dfrac{\partial^2 F(y_1, y_2)}{\partial y_1 \partial y_2} \right)^2 > 0, \\[2ex] \dfrac{\partial^2 F(y_1, y_2)}{\partial {y_1}^2} > 0 . \end{cases} \tag{5}$$

According to [11], setting $y_k = y_1$ and $y_L = y_2$, we obtain the coordinates of the triple dislocation nodes $K(0; y_k; 0)$ and $L(0; y_L; 0)$ corresponding to the equilibrium state of the dislocation configuration for the given value of the applied stress.

In the model [5, 6], the change in the length of dislocation junction and its destruction as a result of rearrangement of the entire dislocation configuration under stress was investigated. In this case, arbitrary intersections of reacting dislocations were considered. The ratios of lengths of glissile dislocation segments $\gamma_g = QO / QP$ and forest dislocation segments $\gamma_f = NO/NM$ (Fig. 2) changed within the limits $\gamma_g = 0.1 - 0.9$ and $\gamma_f = 0.1 - 0.9$. Examples of concrete intersections with the indicated values of the parameters γ_g and γ_f are shown in Fig. 2.

As demonstrated in [5, 6, 10–12], the geometry of intersection of reacting dislocations influences both initial length of the junction and the process of junction destruction. The process of dislocation junction destruction with the destruction mechanisms was described in [10–12]. It was revealed that about 8% of dislocation junctions destruct completely under stress. The destruction proceeds by merging of the dislocation nodes K and L. This mechanism is realized at small tilt angles ($\leq 20^\circ$) of the glissile dislocation to the connecting line and values of the parameters $\gamma_g, \gamma_f = 0.7 - 0.9$ [12]. The destruction of the junction provides dislocation motion in the shear zone.

It was revealed that because of the stability loss by one of the right segments (QE or NE), the junction was bypassed by the reacting segment, and the dislocation junction remained non-destroyed; its length was smaller by one-two orders of magnitude than the length of the initial junction. The junction also remained non-destroyed in the case of stability loss by one of the left segments (FM or FP); its length was greater than the length of the initial junction. Non-destroyed junctions provided accumulation of dislocations in the zone, thereby contributing to the density of dislocation debris. At a certain intersection geometry, for example, at $\gamma_g = 0.1$ and $\gamma_f = 0.1$ (Fig. 2*a*), long junctions $\geq 0.9QP$ were formed, where QP is the length of the free segment of the glissile dislocation. They represented strong barriers [11] bounding the shear zone.

2. DETERMINATION OF THE MEAN FREE PATH OF DISLOCATION SEGMENTS

To determine the mean free path, the following components of the loop were chosen: close to the screw dislocation $(\psi = 0-10^\circ)$ with mixed orientation, close to the 60-degree $(\psi = 55-65^\circ)$, and close to the edge one $(\psi = 80-90^\circ)$. Here ψ is the angle between the dislocation axis and its Burgers vector. We now calculate the mean free path of dislocation segments of different orientations from formula (3), setting the following values of the index: $i = S$ (screw), $i = 60^\circ$ (60-degree), and $i = E$ (edge) components of the loop. Then mean free path of the screw loop component L_S is given by the following expression [8]:

$$L_S = 2(\beta_D^S \beta_r^S \xi\rho)^{-1/2}, \tag{6}$$

where β_r^S and β_D^S are the parameters of the junctions formed by the screw dislocations. The mean free path of the edge components of the loop L_E has the form [8]

$$L_E = 2(\beta_D^E \beta_r^E \xi\rho)^{-1/2}, \tag{7}$$

where β_r^E and β_D^E are the parameters of the junctions formed by the edge dislocations. Similarly, from Eq. (3) we obtain the mean free path for the 60-degree dislocations.

In this work, the following values of the parameters were determined: β_D^S, $\beta_D^{60^\circ}$, and β_D^E – the probabilities of forming long strong dislocation junctions which length $\geq 0.9QP$ for the $[1\,0\,1]$ and $[\bar{1}\,1\,1]$ orientations of the crystal deformation axis. The detailed description of the model is necessitated by its modification for the determination of the given parameters. This is caused by the fact that earlier there was no need to define the dislocation type. The modified model allows the orientation of the reacting segment of the loop to be determined at each calculation step.

Results of calculations for all dislocation reactions with the $[1\,0\,1]$ and $[\bar{1}\,1\,1]$ orientations of the crystal deformation axes are given in Table 1. The value of the shear modulus was $G = 5.46 \cdot 10^4$ MPa, the modulus of the Burgers vector was $b = 2.5 \cdot 10^{-10}$ m, and the dislocation density was $\rho = 10^{13}$ m^{-2}.

Analyzing the results obtain, we note that for the $[1\,0\,1]$ deformation axis, the glissile dislocations close to screw ones did not form long strong dislocation junctions of length $\geq 0.9QP$ in both dislocation reactions. The absence of long strong junctions was also observed for the $[\bar{1}\,1\,1]$ deformation axis (Table 1).

Values of the probability β_r^i of forming dislocation junctions (Table 2) for different components of the loop were obtained in [13] for the simplest model of inter-dislocation interactions. We determine the mean free path from Eq. (3) for the known values of the fraction of forest dislocations $(\xi = 0.5)$ and of the parameters β_r^i and β_D^i (Table 2).

TABLE 1. Probability of Forming Long Strong Junctions by the Indicated Segments of the Dislocation Loops

Reaction type	Reaction equation	Screw $(\psi = 0-10^{o})$	Mixed $(\psi = 55-65^{o})$	Edge $(\psi = 80-90^{o})$
		β_D^S	$\beta_D^{60^\circ}$	β_D^E
$[1\,0\,1]$ orientation of the crystal deformation axis				
3a	$\boldsymbol{BA},d + \boldsymbol{DB},a = \boldsymbol{DA}$	0	0.026	0.017
4a	$\boldsymbol{BA},d + \boldsymbol{DC},a = \boldsymbol{BD}/\boldsymbol{AC}$	0	0.03	0.023
	Average values along the axis	0	0.028	0.02
$[\bar{1}\,1\,1]$ orientation of the crystal deformation axis				
1a	$\boldsymbol{BA},d + \boldsymbol{DB},c = \boldsymbol{DA},c$	0.008	0	0
2a	$\boldsymbol{BA},d + \boldsymbol{CB},a = \boldsymbol{CA},d$	0	0.009	0.007
3a	$\boldsymbol{BA},d + \boldsymbol{DB},a = \boldsymbol{DA}$	0	0.02	0.001
	Average values along the axis	0.003	0.01	0.003

TABLE 2. Mean Free Paths of the Indicated Segments of the Dislocation Loop

Orientation of the deformation axis	Screw $(\psi = 0-10^{\circ})$			Mixed $(\psi = 55-65^{\circ})$			Edge $(\psi = 80-90^{\circ})$		
	β_r^S [13]	β_D^S	L_S	$\beta_r^{60^\circ}$ [13]	$\beta_D^{60^\circ}$	L_{60°	β_r^E [13]	β_D^E	L_E
$[1\,0\,1]$	0.104	0	–	0.257	0.028	$11\cdot10^{-6}$ M	0.27	0.02	$17\cdot10^{-6}$ M
$[\bar{1}\,1\,1]$	0.163	0.003	$40\cdot10^{-6}$ M	0.251	0.01	$18\cdot10^{-6}$ M	0.265	0.003	$32\cdot10^{-6}$ M

The results of calculations demonstrated that for the $[1\,0\,1]$ deformation axis, strong long junctions are formed by dislocation segments with orientations close to 60-degree or edge ones. For the $[\bar{1}\,1\,1]$ deformation axis, dislocation segments with orientations of all examined types form long strong dislocation junctions whose length is greater than $0.9QP$.

CONCLUSIONS

Results of modeling for the modified model of inter-dislocation of interactions have allowed us to conclude the following:

1) For the $[1\,0\,1]$ orientation of the deformation axis, the screw components of the loop did not form long strong dislocation junctions representing the barriers bounding the shear zone.

2) The greatest number of long junctions was formed by dislocations with orientation close to 60-degree one; hence, they had the least mean free path.

3) For the $[\bar{1}\,1\,1]$ orientation of the deformation axis, the screw components of the loop had the longest mean free path.

Thus, it should be noted that the change in the orientation of the crystal deformation axis influenced strongly the mean free path of different segments of the dislocation loop.

REFERENCES

1. R. Berner and H. Kronmüller, Plastische Verformung von Einkristallen, Springer, Berlin (1965).
2. L. E. Popov, V. S. Kobytev, and T. A. Kovalevskaya, Plastic Deformation of Alloys [in Russian], Metallurgiya, Moscow (1984).
3. R. I. Kurinnaya, L. V. Ganzya, and L. E. Popov, Russ. Phys. J., **25**, No. 8, 710–713 (1982).
4. J. Schoeck and R. Frydman, Phys. Status Solidi (b), **53**, 661–674 (1972).
5. R. I. Kurinnaya, M. V. Zgolich, and V. A. Starenchenko, Russ. Phys. J., **47**, No. 7, 705–712 (2004).
6. V. A. Starenchenko, M. V. Zgolich, and R. I. Kurinnaya, Russ. Phys. J., **52**, No. 3, 245–251 (2009).
7. V. A. Starenchenko, R. I. Kurinnaya, D. N. Cherepanov, M. V. Zgolich, and O. V. Selivanikova, IOP Conf. Series: Mater. Sci. and Eng., **71**, 012080 (2015); DOI: 10.1088/1757– 899X/71/1/012080.
8. R. Kurinnaya, M. Zgolich, D. Cherepanov, V. Starenchenko, O. Selivanikova, and M. Matveev, AIP Conf. Proc., **1800**, 030006-1–030006-7 (2015); DOI: 10.1063/1.4973038.
9. R. I. Kurinnaya, M. V. Zgolich, and V. A. Starenchenko, Fund. Probl. Sovr. Materialoved., **13**, No. 4, 456–461 (2016).
10. M. V. Zgolich, R. I. Kurinnaya, and V. A. Starenchenko, Vestn. Tambovskogo Univ. Ser. Estestv. Tekh. Nauki, **18**, No. 4, Part 2, 1554–1555 (2013).
11. V. A. Starenchenko, N. N. Belov, Yu. V. Solovieva, *et al*., Mathematical Modeling from Interdislocation Interactions to Macroscopic Deformation [in Russian], Publishing House of Tomsk State University (2015).
12. R. Kurinnaya, M. Zgolich, V. Starenchenko, and G. Sadritdinova, AIP Conf. Proc., **1698**, 040001-1–040001-6 (2016); DOI: 10.1063/1.4937837.
13. R. I. Kurinnaya, in: Mathematical Models of Plastic Deformation, Inter-University Scientific-Technical Digest, Publishing House of Tomsk Polytechnic University, Tomsk (1989), pp. 58–65.